Modeling of tunnel lining deformation due to face instability

Herbert Walter
Consultant, Salzburg, Austria

Charles James Coccia, Robert B. Wallen, Hon-Yim Ko, John Scott McCartney
University of Colorado, Boulder, Colorado, USA

ABSTRACT: This study presents the results from a series of centrifuge modelling experiments on tunnels in dry sand, performed to evaluate the role of tunnel face movements on the deformation of the tunnel lining and the collapse of the overburden sand. Specifically, a half-space tunnel was modelled, in which a stepper motor was used to control the displacement of the tunnel face during centrifugation under a constant acceleration level. Three tunnel configurations were evaluated, including a full-face excavation, staged excavation, and a full-face excavation with an unlined section. The tunnel models were designed to permit free deformations of the lining and soil during spin-up and face displacement. Narrow shear bands were noticed in all tests, with wider bands in the staged excavation tunnels. Moments and shear forces within the tunnel lining indicate that construction staging leads to the lowest earth pressure and lining deformation with tunnel face movement.

1 INTRODUCTION

Field experience indicates that the tunnel face is the element most susceptible to collapse during construction of tunnels in soil or rock using the New Austrian Tunnelling Method (NATM) or Shotcrete Lining Tunnelling (SCL). The combination of high stress concentrations near the tunnel face and a time-dependent increase in strength of new shotcrete both contribute to possible deformations in the tunnel lining if construction staging is not properly controlled. Extreme face displacements can lead to tunnel cave-ins and associated surface deflections, which are especially a problem for tunnels constructed in urban areas. Despite the high potential for loss of life and property, the safety factors currently used in tunnel design are mainly based on experience, with little basis in field measurements or validated modelling results. The main aim of this paper is to develop tunnel performance data which can be used in the future to validate numerical models and develop rational safety factors for tunnel construction using NATM. Specifically, the behaviour of tunnel models was evaluated in the 400g-ton geotechnical centrifuge at the University of Colorado at Boulder.

Previous work on centrifuge modelling of tunnels was focused on face stability and face support measures (Meguid *et al*. 2008). With very few exceptions (König *et al.* 1991), the tunnel lining was rigid and could not follow the soil deformation during spin-up of the centrifuge. The unique aspect of this study is that the tunnel evaluated had stiffness values that are appropriately scaled based on prototype NATM tunnels. This paper focuses on the model setup, test procedures, instrumentation used to evaluate liner and soil deformations, and changes in liner normal forces and moments during tunnel face movement.

2 DESIGN CONSIDERATIONS

2.1 *Model Size and Dimensions*

The centrifuge-scale tunnel model considered in this study was designed to represent common situations of soil tunnelling in urban environments such as those in the Vienna metro system. The diameters of the tunnels in this system constructed using NATM typically range from about 6 m (single track metro tunnel) to 14 m (3-lane road tunnel).

Numerical studies have shown that the influence of boundary conditions on the face stability can be neglected when the width of the model is larger than 2 tunnel diameters (2D), the lower boundary is more than 0.5D below the invert, the longitudinal extension of the model ahead of the face is more than 2D and the longitudinal extension of the tunnel back from the face is more than 0.5D (Ruse 2004). In order to meet these size requirements to reduce the impacts of boundary conditions on the tunnel behaviour, a centrifuge container with inner dimensions 762 mm × 305 mm × 406 mm (L×B×H) was used in

this study. A picture of the centrifuge model container and tunnel model is shown in Figure 1. The box has three walls and a base constructed from aluminium plates having a thickness of 12.7 mm. The other wall is acrylic with a thickness of 38.1 mm. The acrylic wall was selected to represent the vertical plane of symmetry of the tunnel. A brace was attached to the box to minimize lateral deformation of the acrylic under high g-levels.

Figure 1. Model container showing tunnel configuration.

In order to model the dimensions and overburdens of typical shallow tunnels in an urban setting with this model container geometry, a g-level of 70 was selected. This g-level permitted a centrifuge model tunnel having an inner diameter of 102 mm to be geometrically similar to a prototype tunnel having an inside diameter of 7.0 m. Although tunnels with overburdens of 1D and 2D were evaluated, only the results from tests on tunnels with an overburden of 1D are discussed in this paper. In all tests, the invert (bottom) of the tunnel is located 140 mm above the inside of the base of the container box.

2.2 *Materials*

2.2.1 *Soil*

Dry Ottawa F75 sand was used in all of the experiments. This is a silica sand, with a uniform particle size distribution (C_u = 1.6), a maximum particle size of 0.2 mm and a relatively small fines content of 0.5%. The sand has a friction angle of 30 degrees at a dry unit weight of 17.2 kN/m^3. Although dry sand is not representative of most field settings, it can be placed in relatively uniform conditions in centrifuge models. It also permits repeatable material properties to be obtained from test to test, allowing straightforward parametric analyses to be performed. As the goal of the test performed as part of this study was to validate numerical models, repeatable soil properties simplify calibration of tunnel parameters.

Sand was also used as they represent a worst-case situation for sudden failure conditions, with mobilization of failure surfaces up to the surface. Cohesive soils are more ductile, so deformations can be detected and mitigated in the field to avoid failure.

2.2.2 *Tunnel Lining*

The strength and stiffness of shotcrete increase significantly during the first hours after application. Cast acrylic was found to have stiffness similar to shotcrete at an age of around 6 hours. Cast acrylic has a Young's modulus of 3.1 GPa, a Poisson's ratio of 0.35 and a density of 1190 kg/m^3. A difference is that the strain at rupture for the acrylic is more than 6%, which is much larger than that of shotcrete. However, because this study involves evaluation of the tunnel deformations caused by face deformations, the soil is expected to collapse in the centrifuge models before rupture of the tunnel lining.

2.3 *Tunnel Experimental Setup*

2.3.1 *General Setup Explanation*

Tunnels constructed in the field with the NATM rarely fail during excavation because a number of precautions are taken to stabilize the face, including forepoling, face bolts, sealing of the soil with shotcrete, and combinations of these measures. In the experimental setup, these precautions are neglected. Instead of modelling the excavation process of the tunnel, the approach in this study is to evaluate the stresses in the lining system during (backward) movement of a rigid support of the tunnel face

2.3.2 *Tunnel lining*

For prototype tunnels having a diameter of 7.0 m, a shotcrete lining thickness between 25 and 40 cm is frequently chosen in practice. This corresponds to a model lining thickness of 3.6 to 5.7 mm. A slightly thinner lining thickness of 3.18 mm was selected for the current setup as it is expected to provide worst-case deformation behaviour.

The acrylic side wall of the container box is assumed to be a plane of symmetry, so a restraint was enforced on the movement of the tunnel lining. Specifically, displacements of the tunnel lining normal to the symmetry plane are forced to be zero, and only rotation and sliding with vectors parallel to the symmetry plane are permitted. A sliding mechanism was developed to maintain this boundary condition. The sliding mechanism, shown in Figure 2(a), consists of 15 mm sheets of acrylic bonded to the half-tunnel lining which fit beneath an acrylic guide sleeve attached to the acrylic pane of the container box. Because the sheets may alter the bending stiffness of the tunnel lining, fins were cut into the sheets within a length of 2D from the tunnel face, as shown in Figure 2(b). The sheets of acrylic and the guide sleeve were greased so that the tunnel could freely slide along the acrylic pane of the container. The fins were omitted over the tunnel lining in the last 5 cm from the face to permit displacement of the tunnel face. No connection was provided between the end of the tunnel and the aluminium side of the container wall (on the direction opposite from the face). The gap between the tunnel and the alumin-

ium container was sealed using foam sealant tape, typically used to seal windows or door jambs. A stop in the guide sleeve prevents longitudinal movement of the tunnel lining. Pictures of the tunnel during centrifuge testing indicate that the sliding mechanism adequately provides the required boundary conditions for the tunnel lining.

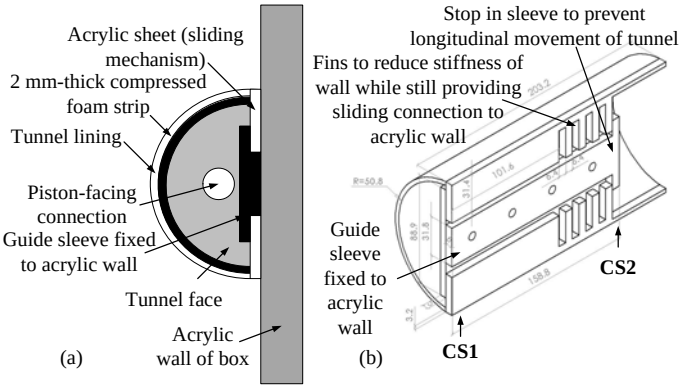

Figure 2. Tunnel lining: (a) Cross-section; (b) Isometric.

A picture of the tunnel model used to simulate full-face excavations is shown in Figure 3(a). This picture is from an early test; the load cell was moved to the back of the piston connected to the wall face in order to minimize bending effects on the measured load. In some of the tests, an unlined section of shotcrete at the face of the tunnel having a length of 25 mm (0.5D) was modelled, shown in Figure 3(b). A thin (0.25 mm) cellophane strip was used to simulate very young shotcrete at the face which has not yet developed measurable stiffness and strength. The tape serves to keep the sand in place as the face is withdrawn. Other tests were performed to assess the impact of staged construction on wall deformations, using the lining shown in Figure 3(c). To create this lining system, an acrylic tube was cut to simulate a top heading which has been excavated further than a bottom heading, a common technique in NATM practice. The length of the top heading is equal to 50 mm (1D). Both the top and bottom faces of the tunnel moved as a single unit during testing.

2.3.3 *Tunnel face*

The tunnel face was modelled as a rigid element, with displacement-controlled behaviour. This is not realistic when modelling actual NATM tunnel faces, which are relatively flexible. However, the emphasis of this study is the impact of tunnel face movement on the lining and collapse of the overburden sand. The tunnel face used to simulate full-face excavation was a 48 mm-diameter half-circle acrylic disc having a thickness of 12.5 mm. Sponge foam having a thickness of 2 mm was used to bridge the gap between the face and lining. This approach was found to provide both a sand-tight connection while still maintaining low sliding friction as well as allowing displacements of the lining relative to the acrylic disk. Saran wrap was placed around the tunnel lining and face to minimize sand leakage into any cracks. Slack was provided in the Saran wrap so that it didn't interfere with movement of the tunnel lining.

The model tunnel face is connected to a metal rod supported by roller bearings. A load cell is connected in series to the metal rod and the wall face to permit measurement of the lateral earth pressure during movement of the tunnel face. The metal rod is connected to a stepper motor, shown in Figure 1, which is used to pull the tunnel face backward at a constant displacement rate. This is expected to simulate the removal of material from the face of the tunnel at a constant rate. This is intended to simulate a failure situation that likely would not occur in the field. Specifically, if tunnelling were being performed in dry sand in the field, it is likely that the sand would be stabilized prior to excavation using the NATM method. Nonetheless, this modelling exercise permits an understanding of the mechanisms of tunnel deformation during collapse of a cohesionless soil.

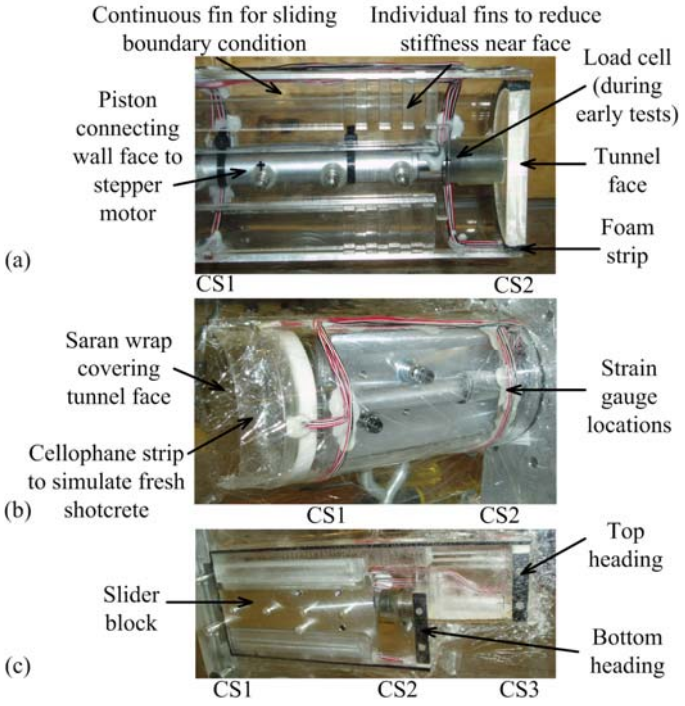

Figure 3. Pictures of the tunnel lining: (a) Full-face tunnel; (b) Full-face tunnel with unlined section; (c) Staged excavation.

3 INSTRUMENTATION

As mentioned above, the face pressure is measured using a load cell mounted on the rod connecting the stepper motor with the tunnel face. The rod was placed between a series of bearings connected at different locations along the acrylic pane of the container to prevent bending forces from being transmitted to the load cell, while permitting free movement of the rod. The load measured with the load cell requires the soil to deform as the face is withdrawn to maintain active earth pressure conditions on the face. Arching in the soil may lead to inaccuracies in the measured force, so the load cell results are mainly useful for comparative purposes.

Deformation of the tunnel lining was monitored using epoxy-bonded strain gages at the ceiling, middle, and invert locations for two cross-sections in all of the three tunnel lining types, labelled as CS1 and CS2 in Figure 2(b). Pairs of strain gages at the intrados and at the extrados were used to allow the calculation of moments and normal forces. Strain gages were only installed in the circumferential direction at CS1, as it was assumed that longitudinal stresses here were small. Strain gages were installed in the circumferential and longitudinal directions at CS2 and CS3. Only the circumferential strain gauge results are presented in this paper.

The location of cross section CS1 was 25 mm from the side wall. The strain gauges at CS1 are intended for observation of tunnel lining deformation due to overburden effects, but not face displacement effects. The location of cross section CS2 was chosen as close as possible to the tunnel face for the full-face excavation tunnels, in order to measure deformations during movement of the tunnel face. For the tunnels with staged excavation, strain gauges were installed at an additional cross section, CS3, close to the face of the top heading [Figure 3(c)].

As a back-up for the deformation measurement system, digital image analysis was used. A digital camera (5 Megapixel, b/w) was mounted to the platform of the centrifuge. Images of the symmetry plane were obtained every second during the tests. LabView software was used to track the movement of planes (*e.g.*, tunnel face and tunnel lining). In addition, these images were used to qualitatively assess the deformation in the soil layer above the tunnel during the tests. In these images, one pixel corresponds to about 0.4 mm.

4 CENTRIFUGE TESTING PROCEDURES

The centrifuge model was prepared by removing the back of the container box, adding a temporary lid to the container, and turning the box so that the acrylic pane faced downwards. The tunnel model was assembled on the sliding mechanism on the acrylic pane, and was covered with Saran wrap. Lines of green sand were placed on the acrylic pane of the container to aid in the observation of shear band development. The sand was then pluviated into the container from a height of 2.5 m, resulting in a dry unit weight of 17.2 kN/m³. The opposite container box wall was carefully replaced after pluviation and the container was returned to its upright position. Although this procedure causes some disturbance of the primary stress state before spin-up, it permits control of the sand density on the top and bottom of the tunnel. The height of the overburden was regulated by adding styrofoam spacers.

During spin-up of the tunnel model, the tunnel face position is maintained stationary. After reaching the target g-level of 70 g, the tunnel face was slowly retracted at a rate of 12.5 μm/s. This speed simulates a prototype-scale displacement rate of 0.875 mm/s. This speed was selected to permit an ample number of pictures during movement of the tunnel face. The sliding mechanism allows a tunnel face displacement of 20 mm. To expedite the test, the speed of the stepper motor was increased by a factor of 3 after shear bands were observed to fully extend to the sand surface. Movement of the tunnel face beyond this point led to formation of a surface funnel but minimal tunnel lining deformations.

5 TEST RESULTS

5.1 *Soil Deformation*

Evaluation of pictures of the soil profile during movement of the tunnel face shows the development of very pronounced shear bands during piston movement, as shown in Figure 4. In all of the tests, the observed shear bands were very steep. The resulting funnel at the surface was always narrow and smaller in diameter than the tunnel diameter for a face displacement of 20 mm.

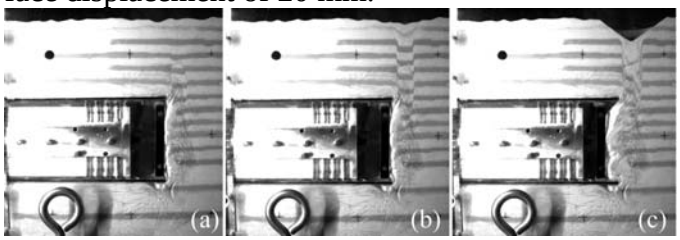

Figure 4. Pictures during centrifugation showing progression of overburden collapse during withdrawal of tunnel facing.

There is a pronounced difference in the shapes of the shear bands and funnel sizes between the different tunnel lining sections, as observed in Figure 5. Staged excavation leads to a surface funnel that is more elliptical than that for a full face excavation. Staged excavation with an unlined section leads to a wider shear band than the tunnels without an unlined section. The same observation was made for full-face excavations with an unlined section.

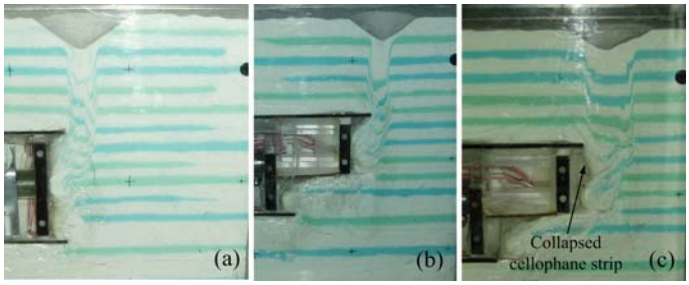

Figure 5. Deformation patterns at failure for tunnels with: (a) Full-face excavation; (b) Staged excavation; (c) Staged excavation with an unlined section.

5.2 *Face Pressure and Tunnel Lining Deformation*

The face pressure as a function of face displacement for a tunnel with a full-face excavation is

shown in Figure 6(a). For a tunnel with a diameter D and an overburden of D, the active earth pressure on the tunnel face should be $1.5\gamma DK_a$, or 54 kPa. The measured pressure is lower than this value, as expected if friction between the tunnel face and acrylic pane were present. Arching effects and bending of the load cell could have also contributed to a lower face pressure. The displacement of the piston resulted in an increase of load cell force immediately after start of the movement; the pressure kept rather constant afterwards. (At reaching the maximum displacement, the pressure dropped, probably caused by some locking of the piston or the saran wrap.)

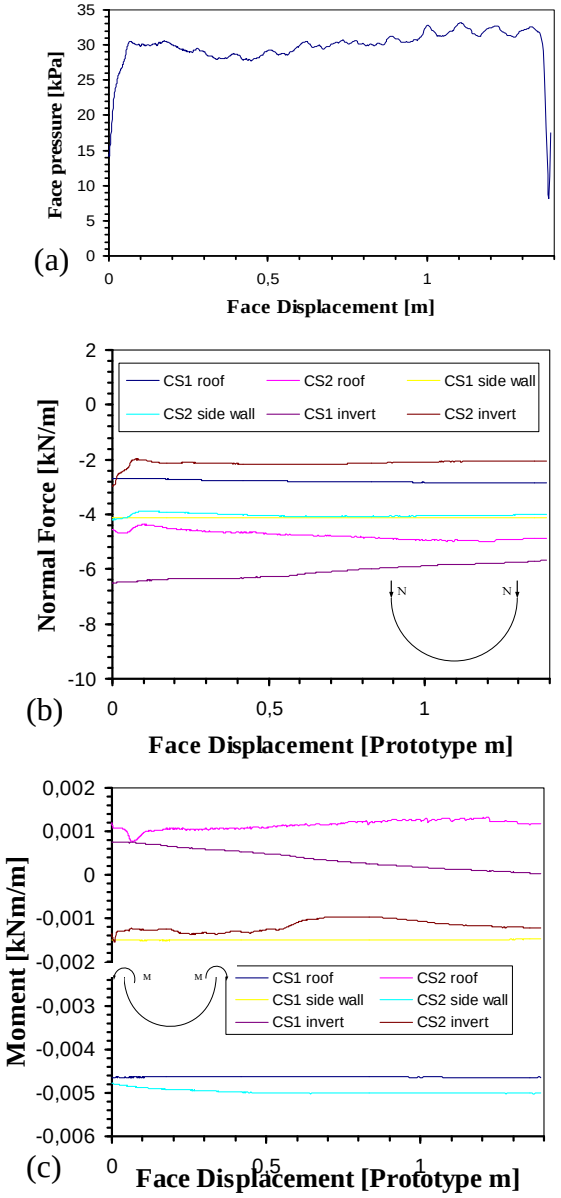

Figure 6. Results for a full-face tunnel.

The strain measurements at the roof, side wall, and invert of the tunnel were synthesized to calculate the moments and normal forces (centrifuge scale) in the tunnel lining, shown in Figure 6(b) and 6(c). These values were calculated assuming plane stress conditions, a centrifuge-scale lining thickness of 3.175 mm, and the elastic properties of acrylic listed in Section 2.2.2. The normal forces and moments at zero displacement represent the effects of the at-rest centrifugal acceleration on the tunnel lining. Only slight changes in the normal forces and moments were noted due to the tunnel face displacement. Higher compressive forces were noted near the tunnel face, with the highest forces in the invert, as expected. The moment at the roof of the tunnel near the face (CS2) was higher than in CS1, which indicates squeezing of the tunnel near the face. The moment in CS2 was lower in the middle and similar at the invert.

The face pressure in a tunnel with a full-face excavation, but with an unlined section, Figure 7(a), shows a drop in earth pressure at a higher face displacement for this tunnel. Similar to the other full-face excavation shown in Figure 6(b), the normal forces in Figure 7(b) were higher in the cross section near the tunnel face. The magnitudes of the normal forces were slightly higher than in the fully-lined tunnel. The trends in the moments in Figure 7(c) are also similar to those shown in Figure 6(c); changes during the piston movement are less pronounced.

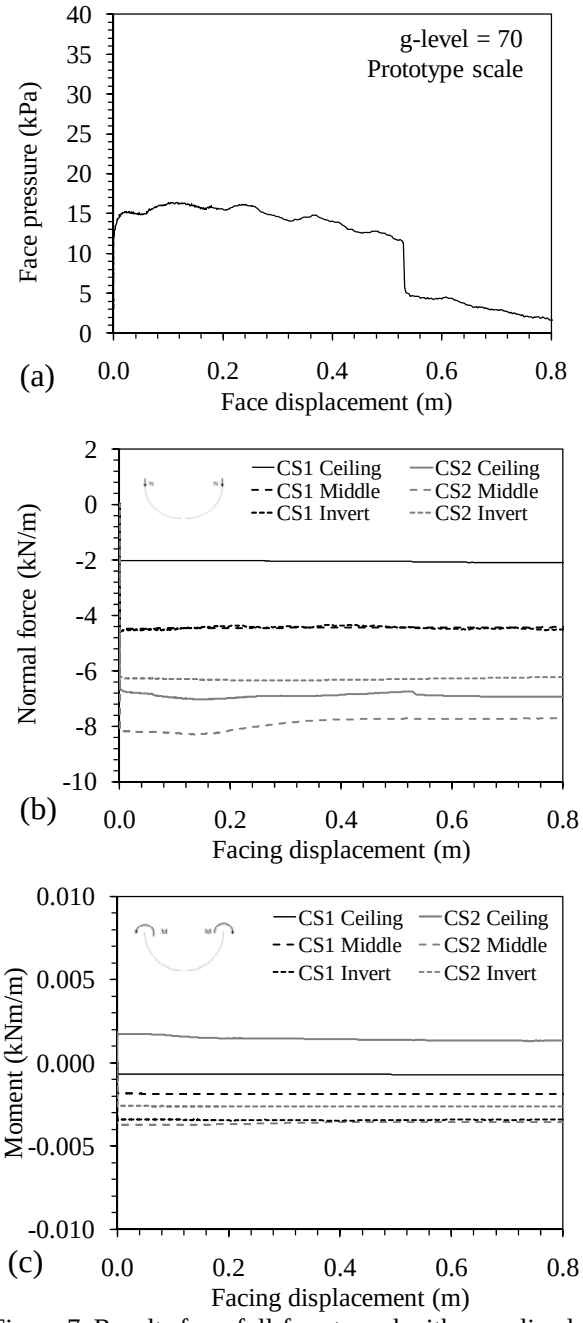

Figure 7. Results for a full-face tunnel with an unlined section.

The face pressure in the tunnel with staged excavation shown in Figure 8(a) is the lowest of the three tunnel lining systems investigated. This may be due to arching of sand around the top heading, leading to less pressure on the bottom heading. A steady decrease in face pressure was measured in this test. The trends in normal forces in Figure 8(b) are different for this tunnel, with nearly tensile forces at the middle of the top heading near the face (CS3) and the lowest normal forces in the ceiling near the top heading. This may be due to the discontinuity in the tunnel lining at the middle of the tunnel. The magnitudes of the normal forces are the smallest of the three tunnel lining systems. Face displacement had the greatest impact on normal forces in the top heading. The moments in the tunnel lining with staged excavation at CS2, except in the middle, were the smallest observed [Figure 8(c)]. These observations are consistent with those of Walter *et al.* (2010).

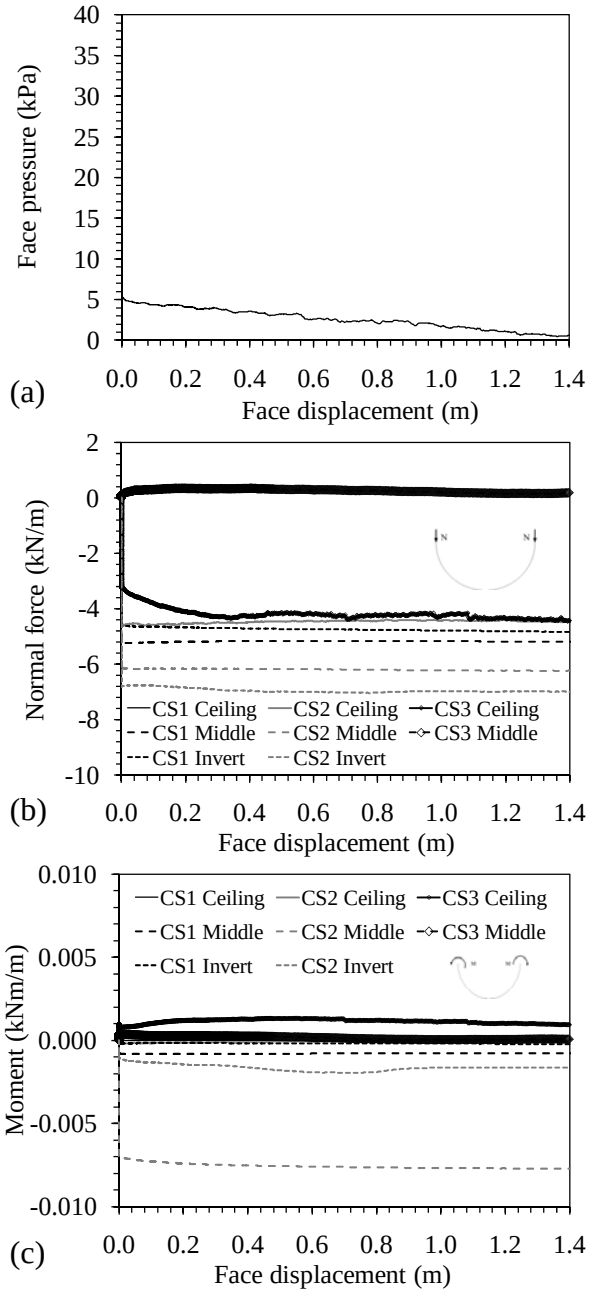

Figure 8. Results for a tunnel with staged excavation.

5.3 *Discussion of Results*

An important aspect of tunnel face stability, the face pressure, was not characterized as desired. Although efforts were made to minimize the effects of bending on the load cell, the results indicate that even small bending caused errors which could not be avoided. A load cell with little sensitivity to off-axis loading is needed to improve the accuracy of face pressure readings with sufficient redundancy. Because the earth pressure values under investigation are relatively small, the effect of friction between the face and tunnel lining can have a considerable effect on the load cell readings. Another factor which may have impacted the measured deformation of the tunnel lining is friction in the sliding mechanism, between the insulating foam on the face and the lining, and between the lining and container.

6 CONCLUSIONS

The development and evaluation of centrifuge models of tunnels with deformable lining were described in this paper. The boundary conditions were controlled satisfactorily to model deformable tunnels during movement of the tunnel face. The flexible tunnel lining equipped with cross sections of epoxy bonded strain gages provided insight into soil-tunnel interaction during face movement. Tunnels with staged construction showed the lowest face pressures and the lowest magnitude of normal forces and moments in the tunnel lining. Tunnels with an unlined section had the most pronounced collapse of the overburden soil during face displacement.

7 ACKNOWLEDGEMENTS

The 1st author was supported by the KIRAS program of the Austrian Research Promotion Agency (FFG) and the Austrian Society for Geomechanics (ÖGG). Their support is gratefully acknowledged.

REFERENCES

König, D., Güttler, U. & Jessberger, H. L. 1991. Stress Redistribution during Tunnel and Shaft Construction. In: *Centrifuge 1991*, Boulder, Colorado, p.129-135.

Meguid, M.A., Saada, O., Nunes, M.A. & Mattar, J. 2008. Physical Modeling of Tunnels in Soft Ground: A Review. *Tunnelling and Underground Space Tech. 23*, 185–198.

Ruse, N. 2004. *Räumliche Betrachtung der Standsicherheit der Ortsbrust beim Tunnelvortrieb*, Mitteilung 51 des Instituts für Geotechnik, University Stuttgart.

Walter, H., Coccia, C. J., Ko, H.-Y. & McCartney, J. 2010, Investigation of Tunnel Face Stability Using a Deformable Tunnel Lining with a Centrifuge Model. *GeoFlorida 2010*, West Palm Beach FL, USA. Feb. 20-24, 2010.